J. Korean Math. Soc. **62** (2025), No. 1, pp. 77–96
https://doi.org/10.4134/JKMS.j230587
pISSN: 0304-9914 / eISSN: 2234-3008

MIXED FINITE VOLUME METHOD FOR TWO-DIMENSIONAL MAXWELL'S EQUATIONS

Kwang-Yeon Kim and Do Young Kwak

Abstract. We propose and analyze a mixed finite volume method for the two-dimensional time-harmonic Maxwell's equations which simultaneously approximates the vector field $\boldsymbol{u}$ and the scalar function $\xi = \mu^{-1}\operatorname{curl}\boldsymbol{u}$. The method chooses the lowest-order Nédélec edge element for $\boldsymbol{u}$ and the $P1$ Crouzeix–Raviart nonconforming element for ξ on triangular meshes. It is shown that the method is reduced to a modified $P1$ nonconforming FEM for ξ or a modified edge element method for $\boldsymbol{u}$ by eliminating the discrete variable of $\boldsymbol{u}$ or ξ. After solving the reduced method, the eliminated discrete variable can be recovered from the other one via a simple local formula. Using this feature, we also derive optimal a priori error estimates under weak regularity assumptions and show that the approximation to ξ has a higher-order of convergence in the L^2 norm than the one obtained by direct differentiation of the approximation to $\boldsymbol{u}$ when the exact solution is sufficiently smooth.

1. Introduction

For a bounded polygonal domain $\Omega \subset \mathbb{R}^2$, we consider the following time-harmonic Maxwell's equations with the perfectly conducting boundary condition

$$\begin{cases} \mathbf{curl}(\mu^{-1}\operatorname{curl}\boldsymbol{u}) - \omega^2\epsilon\boldsymbol{u} = \boldsymbol{f} & \text{in } \Omega, \\ \boldsymbol{u}\cdot\boldsymbol{t} = 0 & \text{on } \partial\Omega, \end{cases} \tag{1}$$

where $\boldsymbol{t}$ is the unit tangent vector on $\partial\Omega$ with positive orientation and

$$\operatorname{curl}\boldsymbol{v} = \frac{\partial v_2}{\partial x} - \frac{\partial v_1}{\partial y}, \qquad \mathbf{curl}\,\phi = \left(\frac{\partial\phi}{\partial y}, -\frac{\partial\phi}{\partial x}\right)$$

for a vector field $\boldsymbol{v} = (v_1, v_2)$ and a scalar function ϕ. The vector field $\boldsymbol{u}$ represents the electric field and $\boldsymbol{f} \in (L^2(\Omega))^2$ is a given function due to external

Received November 6, 2023; Revised March 15, 2024; Accepted May 27, 2024.
2020 *Mathematics Subject Classification.* Primary 65N08, 65N30, 65N15.
Key words and phrases. Maxwell's equations, mixed finite volume method, Nédélec edge element, $P1$ nonconforming finite element.
This work was supported by the National Research Foundation of Korea(NRF) grant funded by the Korea government(MSIT) (No. 2021R1F1A1050243).

current sources. The coefficients μ and ϵ represent the magnetic permeability and the electric permittivity, respectively, and are assumed to be scalar functions bounded above and below by positive constants. The parameter ω is a positive constant representing a temporal frequency of the electromagnetic wave.

Let us introduce the space of all square integrable vector fields on Ω with square integrable curls

$$\boldsymbol{H}(\mathrm{curl};\Omega) = \{\boldsymbol{v} \in (L^2(\Omega))^2 : \mathrm{curl}\,\boldsymbol{v} \in L^2(\Omega)\}$$

with the norm defined by

$$\|\boldsymbol{v}\|_{H(\mathrm{curl};\Omega)} = \left(\|\boldsymbol{v}\|_0^2 + \|\,\mathrm{curl}\,\boldsymbol{v}\|_0^2\right)^{1/2}.$$

As usual, $\|\cdot\|_{s,p,D}$ denotes the norm of the Sobolev space $W^{s,p}(D)$ with the shorthand notation $\|\cdot\|_{s,D} = \|\cdot\|_{s,2,D}$ and $\|\cdot\|_s = \|\cdot\|_{s,2,\Omega}$.

It is known that the following Green's formula holds for $\boldsymbol{v} \in \boldsymbol{H}(\mathrm{curl};\Omega)$ and $\chi \in H^1(\Omega)$

$$\int_\Omega \mathrm{curl}\,\boldsymbol{v}\,\chi - \int_\Omega \boldsymbol{v}\cdot\mathbf{curl}\,\chi = \int_{\partial\Omega} \boldsymbol{v}\cdot\boldsymbol{t}\,\chi, \tag{2}$$

where the integral of the right-hand side denotes the duality paring between $H^{-1/2}(\partial\Omega)$ and $H^{1/2}(\partial\Omega)$. The subspace of $\boldsymbol{H}(\mathrm{curl};\Omega)$ satisfying the boundary condition in (1) is denoted by

$$\boldsymbol{H}_0(\mathrm{curl};\Omega) = \{\boldsymbol{v} \in \boldsymbol{H}(\mathrm{curl};\Omega) : \boldsymbol{v}\cdot\boldsymbol{t} = 0 \text{ on } \partial\Omega\}.$$

Then the variational formulation of (1) is to find $\boldsymbol{u} \in \boldsymbol{H}_0(\mathrm{curl};\Omega)$ such that

$$\int_\Omega \mu^{-1}\,\mathrm{curl}\,\boldsymbol{u}\,\mathrm{curl}\,\boldsymbol{v} - \omega^2\int_\Omega \epsilon\boldsymbol{u}\cdot\boldsymbol{v} = \int_\Omega \boldsymbol{f}\cdot\boldsymbol{v} \tag{3}$$

for all $\boldsymbol{v} \in \boldsymbol{H}_0(\mathrm{curl};\Omega)$. Throughout the paper we assume that $\omega^2 \neq 0$ is not an interior Maxwell eigenvalue so that this problem is uniquely solvable [17, 24].

The problem (1) can be rewritten as the first-order mixed system

$$\begin{cases} \xi = \mu^{-1}\,\mathrm{curl}\,\boldsymbol{u} & \text{in } \Omega, \\ \epsilon^{-1}\,\mathbf{curl}\,\xi - \omega^2\boldsymbol{u} = \epsilon^{-1}\boldsymbol{f} & \text{in } \Omega, \\ \boldsymbol{u}\cdot\boldsymbol{t} = 0 & \text{on } \partial\Omega, \end{cases} \tag{4}$$

where the scalar function ξ represents the z component of the magnetic field which is perpendicular to the electric field $\boldsymbol{u}$. By taking the curl of the second equation in Ω and the tangential component of the same equation on $\partial\Omega$, the system (4) is reduced to the following second-order self-adjoint indefinite elliptic equation for the scalar function ξ

$$\begin{cases} \mathrm{curl}(\epsilon^{-1}\,\mathbf{curl}\,\xi) - \omega^2\mu\,\xi = \mathrm{curl}(\epsilon^{-1}\boldsymbol{f}) & \text{in } \Omega, \\ \epsilon^{-1}\,\mathbf{curl}\,\xi\cdot\boldsymbol{t} = \epsilon^{-1}\boldsymbol{f}\cdot\boldsymbol{t} & \text{on } \partial\Omega. \end{cases}$$

The corresponding variational formulation is to find $\xi \in H^1(\Omega)$ such that

$$a(\xi, \chi) = F(\chi) \qquad \forall \chi \in H^1(\Omega), \tag{5}$$

where

$$a(\xi, \chi) = \int_\Omega \epsilon^{-1} \,\mathbf{curl}\, \xi \cdot \mathbf{curl}\, \chi - \omega^2 \int_\Omega \mu\, \xi \chi, \tag{6}$$

$$F(\chi) = \int_\Omega \epsilon^{-1} \boldsymbol{f} \cdot \mathbf{curl}\, \chi. \tag{7}$$

It was shown in [6, Lemma 3.2] that the problem (5) has a unique solution when $\omega^2 \neq 0$ is not an interior Maxwell eigenvalue. Moreover, the following stability estimate holds

$$\|\xi\|_1 \leq C \|\boldsymbol{f}\|_0. \tag{8}$$

The well-known $H(\mathrm{curl})$-conforming edge elements of Nédélec [26, 27] are based on the primal formulation (3) and have been analyzed in [17, 23–25, 32], just to name a few. Nonconforming and discontinuous FEMs have also been developed in [7–9, 16, 18, 19, 22, 28, 29] (see also the references therein). On the other hand, the authors of [6] proposed a non-traditional FEM using the Hodge decomposition for divergence-free vector fields. This method finds a numerical approximation of $\boldsymbol{u}$ by solving some Dirichlet and Neumann problems for the Laplace operator including (5). For example, one obtains a piecewise constant approximation of $\boldsymbol{u}$ and a continuous piecewise $P1$ approximation of ξ when $P1$ conforming FEMs are used. We remark that H^1-conforming Lagrange finite elements may converge to a wrong solution for (3), unless $\boldsymbol{u} \in (H^1(\Omega))^2$; see, for example, the recent paper [1] and references therein for more details about the use of H^1-conforming Lagrange finite elements based on some regularization or special triangulations.

The aim of this work is to propose and analyze a mixed finite volume method directly based on the mixed system (4). This method seeks to find the numerical approximations $\boldsymbol{u}_h \approx \boldsymbol{u}$ in the lowest-order edge element of Nédélec and $\xi_h \approx \xi$ in the $P1$ nonconforming element of Crouzeix and Raviart. The discretization of (4) is simply done by following the idea of the finite volume box scheme of Courbet and Croisille [13] which was originally developed for the Poisson equation in the mixed form. The main feature of the mixed finite volume method is that it can be readily reduced to either a modified $P1$ nonconforming FEM of (5) or a modified edge element method of (3). More precisely, one can get a matrix system for ξ_h similar to (5) by eliminating $\boldsymbol{u}_h$ locally, and after solving this matrix system, recover $\boldsymbol{u}_h$ from ξ_h via a simple local formula. It is also possible to first eliminate ξ_h and recover it from $\boldsymbol{u}_h$ computed by solving a matrix system similar to (3). This facilitates the derivation of a priori error estimates as well as the implementation of the numerical method. Besides, the mixed finite volume method not only provides an $H(\mathrm{curl})$-conforming approximation of $\boldsymbol{u}$ but also more accurate approximation of $\xi = \mu^{-1} \operatorname{curl} \boldsymbol{u}$ than the standard lowest-order edge element. We refer to [12, 13, 20] for a discussion about other advantages of the mixed finite volume method in the context of the Poisson equation. Our method is similar to that of [6] as approximation of $\boldsymbol{u}$ can be obtained from approximation of ξ computed by solving the Neumann problem (5), but is conceptually more straightforward and easier to implement.

We will derive a priori error estimates for the mixed finite volume method under the weak regularity assumption that $\boldsymbol{u} \in (H^s(\Omega))^2$ and $\xi \in H^s(\Omega)$ for $0 < s \leq 1$, which is known to hold under mild conditions on the coefficients μ, ϵ and the source term $\boldsymbol{f}$; see Remarks 5.2-5.3 for more details on the regularity of $\boldsymbol{u}$ and ξ. The crucial part of the analysis is to establish stability and optimal H^1 and L^2 error estimates for the (modified) $P1$ nonconforming FEM of the problem (5). In the classical error analysis using Green's formula (2), it is necessary to introduce the Nédélec interpolation operator Π_h which is known to satisfy the estimate $\|\boldsymbol{u} - \Pi_h \boldsymbol{u}\|_0 \leq Ch^s \|\boldsymbol{u}\|_s$ only for $\frac{1}{2} < s \leq 1$. We avoid the use of Π_h by adopting the argument of Carstensen et al. [10] based on use of an enriching operator for analyzing the $P1$ nonconforming FEM of second-order elliptic equations. The $H(\mathrm{curl})$ error estimate of $\boldsymbol{u}_h$ follows in a straightforward way from the error estimates of ξ_h using the local recovery formula for $\boldsymbol{u}_h$.

The rest of the paper is organized as follows. In Section 2 we introduce some preliminary results and notation about the lowest-order edge element of Nédélec and the $P1$ nonconforming element of Crouzeix and Raviart. In Section 3 we define the mixed finite volume method and describe how it can be implemented. We establish the stability estimates of the mixed finite volume method in Section 4 and then derive the a priori error estimates in Section 5. Finally, in Section 6 some numerical results are reported to support the theoretical results.

2. Preliminaries

Suppose that $\mathcal{T}_h$ is a shape-regular triangulation of Ω into triangles such that $\overline{\Omega} = \bigcup_{K \in \mathcal{T}_h} \overline{K}$. The set of all edges of $\mathcal{T}_h$ is denoted by $\mathcal{E}_h = \mathcal{E}_h^0 \cup \mathcal{E}_h^\partial$, where $\mathcal{E}_h^0$ and $\mathcal{E}_h^\partial$ consist of all interior and boundary edges, respectively. For a triangle $K \in \mathcal{T}_h$, we denote the diameter of K by h_K, the area of K by $|K|$, and the centroid of K by (x_K, y_K). The mesh size of $\mathcal{T}_h$ is defined as $h = \max_{K \in \mathcal{T}_h} h_K$. For an edge $e \in \mathcal{E}_h$, we denote the length of e by $|e|$.

For approximation of the vector variable $\boldsymbol{u}$ and the scalar variable ξ, we choose the lowest-order edge element of Nédélec [26] and the $P1$ nonconforming element of Crouzeix and Raviart [14] defined by

$$
\begin{aligned}
\boldsymbol{V}_h &= \{\boldsymbol{v}_h \in \boldsymbol{H}(\mathrm{curl};\Omega) : \boldsymbol{v}_h|_K \in (\mathbb{P}_0(K))^2 \oplus (y, -x)\mathbb{P}_0(K) \ \ \forall K \in \mathcal{T}_h\},\\
\boldsymbol{V}_h^0 &= \boldsymbol{V}_h \cap \boldsymbol{H}_0(\mathrm{curl};\Omega),\\
N_h &= \{\chi_h \in L^2(\Omega) : \chi_h|_K \in \mathbb{P}_1(K) \ \ \forall K \in \mathcal{T}_h,\\
&\qquad \text{and } \textstyle\int_e \chi_h \text{ is continuous for every } e \in \mathcal{E}_h^0\},
\end{aligned}
$$

where $\mathbb{P}_r(K)$ denotes the space of all polynomials of degree at most r on K. Note that the two-dimensional edge element is simply obtained by a $90°$ rotation of the Raviart–Thomas element.

It is important to observe that the degrees of freedom of both $\boldsymbol{V}_h$ and N_h are associated with the edges of $\mathcal{T}_h$. The tangential component of $\boldsymbol{v}_h \in \boldsymbol{V}_h$ is constant on every edge $e \in \mathcal{E}_h$ and continuous across every interior edge $e \in \mathcal{E}_h^0$. This fact leads to the following set of degrees of freedom for $\boldsymbol{V}_h$

$$\left\{ \frac{1}{|e|} \int_e \boldsymbol{v}_h \cdot \boldsymbol{t}_e : e \in \mathcal{E}_h \right\},$$

where $\boldsymbol{t}_e$ is a fixed unit tangent vector on e. Similarly, in view of the weak continuity imposed on N_h, the degrees of freedom for N_h are chosen to be

$$\left\{ \frac{1}{|e|} \int_e \chi_h : e \in \mathcal{E}_h \right\}.$$

Consequently,

$$\dim \boldsymbol{V}_h^0 = \#\mathcal{E}_h^0, \qquad \dim N_h = \#\mathcal{E}_h,$$

where $\#A$ is the cardinality of a finite set A.

For $K \in \mathcal{T}_h$, we will often use the following expression for $\boldsymbol{v}_h \in \boldsymbol{V}_h$

$$\boldsymbol{v}_h = \overline{\boldsymbol{v}_h} - \frac{1}{2}(\operatorname{curl} \boldsymbol{v}_h)\boldsymbol{r}_h^{\perp}, \tag{9}$$

where

$$\overline{w}|_K = \frac{1}{|K|} \int_K w, \qquad \boldsymbol{r}_h^{\perp}|_K = (y - y_K, -(x - x_K)).$$

For a vector field $\boldsymbol{v} = (v_1, v_2)$, the integral average operator is applied componentwise, i.e., $\overline{\boldsymbol{v}} = (\overline{v_1}, \overline{v_2})$.

The curl operator applied in a piecewise manner to functions of $H^1(\Omega) + N_h$ will be denoted by $\mathbf{curl}_h$. The bilinear form $a(\cdot,\cdot)$ and the linear functional $F(\cdot)$ defined in (6)-(7) are naturally extended to functions of $H^1(\Omega) + N_h$ by replacing $\mathbf{curl}$ with $\mathbf{curl}_h$. We also define the broken H^1 seminorm and H^1 norm by

$$|\chi|_{1,h} = \| \mathbf{curl}_h \chi \|_0, \qquad \|\chi\|_{1,h} = (\|\chi\|_0^2 + |\chi|_{1,h}^2)^{1/2}.$$

Since μ and ϵ are assumed to be bounded above and below by positive constants, the bilinear form $a(\cdot,\cdot)$ is bounded and satisfies Gårding's inequality for $\eta, \chi \in H^1(\Omega) + N_h$

$$a(\eta, \chi) \le C\|\eta\|_{1,h}\|\chi\|_{1,h}, \qquad a(\chi, \chi) \ge C_1\|\chi\|_{1,h}^2 - C_2\|\chi\|_0^2. \tag{10}$$

In addition, we will assume that the coefficients μ and ϵ satisfy the following estimates for $K \in \mathcal{T}_h$

(11)

$$\|\mu - \overline{\mu}\|_{0,\infty,K} \le Ch, \quad \|\mu^{-1} - \overline{\mu^{-1}}\|_{0,\infty,K} \le Ch, \quad \|\epsilon^{-1} - \overline{\epsilon^{-1}}\|_{0,\infty,K} \le Ch.$$

These are ensured, e.g., if μ, μ^{-1} and ϵ^{-1} are piecewise $W^{1,\infty}$ functions. Above and in what follows, C (with or without a subscript) denotes a generic positive constant independent of the mesh size h (but dependent on μ, ϵ and ω) which may be different at different places.

Now we present the discrete version of Green's formula (2) which will be crucially used in the next section.

Lemma 2.1. *The following identity holds for all* $\boldsymbol{v}_h \in \boldsymbol{V}_h$ *and* $\chi_h \in N_h$

$$\int_\Omega \operatorname{curl} \boldsymbol{v}_h \, \chi_h - \int_\Omega \boldsymbol{v}_h \cdot \mathbf{curl}_h \, \chi_h = \int_{\partial\Omega} \boldsymbol{v}_h \cdot \boldsymbol{t} \, \chi_h. \tag{12}$$

Proof. Using Green's formula (2) on $K \in \mathcal{T}_h$, we obtain

$$\begin{aligned}\int_\Omega \operatorname{curl} \boldsymbol{v}_h \, \chi_h - \int_\Omega \boldsymbol{v}_h \cdot \mathbf{curl}_h \, \chi_h &= \sum_{K \in \mathcal{T}_h} \left(\int_K \operatorname{curl} \boldsymbol{v}_h \, \chi_h - \int_K \boldsymbol{v}_h \cdot \mathbf{curl} \, \chi_h \right) \\ &= \sum_{K \in \mathcal{T}_h} \int_{\partial K} \boldsymbol{v}_h \cdot \boldsymbol{t}_K \, \chi_h,\end{aligned}$$

where $\boldsymbol{t}_K$ is the unit tangent vector on ∂K with positive orientation. Then the result (12) follows by observing that the two integrals on every interior edge of $\mathcal{T}_h$ cancel each other by the continuity properties of $\boldsymbol{V}_h$ and N_h. $\square$

Finally, we introduce an enriching operator $E : N_h \to H^1(\Omega)$ which will be used for error analysis of the $P1$ nonconforming FEM of the problem (5) under the weak regularity assumption $(\boldsymbol{u}, \xi) \in (H^s(\Omega))^2 \times H^{1+s}(\Omega)$ for $0 < s \leq 1$. Enriching operators were used for various purposes in [3–5, 15], where $E\chi_h$ is defined to be the continuous piecewise quadratic polynomial obtained by averaging nodal values of χ_h at every $P2$ Lagrange node of $\mathcal{T}_h$. It was shown in [5, Section 3] that the following approximation property and stability hold

$$\left(\sum_{K \in \mathcal{T}_h} h_K^{-2} \|\chi_h - E\chi_h\|_{0,K}^2 \right)^{1/2} + \|E\chi_h\|_1 \leq C \|\chi_h\|_{1,h} \qquad \forall \chi_h \in N_h. \tag{13}$$

This result is still valid when we modify the values of $E\chi_h$ at midpoints of edges of $\mathcal{T}_h$ in such a way that

$$\int_e E\chi_h = \int_e \chi_h \qquad \forall e \in \mathcal{E}_h.$$

Then, using Green's formula (2) on $K \in \mathcal{T}_h$ yields

$$\int_K \mathbf{curl}(\chi_h - E\chi_h) = 0 \qquad \forall K \in \mathcal{T}_h. \tag{14}$$

In [10], $E\chi_h$ is defined to be the continuous piecewise cubic polynomial which further satisfies

$$\int_K E\chi_h = \int_K \chi_h \qquad \forall K \in \mathcal{T}_h.$$

The proof of [5, Section 3] also applies to this operator so that (13) holds for this operator. We remark that no Dirichlet boundary condition is imposed for $E\chi_h$, as well as for $\chi_h \in N_h$.

3. Mixed finite volume method

By following the idea of the finite volume box scheme of Courbet and Croisille [13] for the Poisson equation, the mixed finite volume method for (4) is defined as follows:

Find $(\boldsymbol{u}_h, \xi_h) \in \boldsymbol{V}_h^0 \times N_h$ such that for all $K \in \mathcal{T}_h$,

$$\int_K \xi_h = \int_K \mu^{-1} \operatorname{curl} \boldsymbol{u}_h, \qquad \int_K (\epsilon^{-1} \operatorname{\mathbf{curl}} \xi_h - \omega^2 \boldsymbol{u}_h) = \int_K \epsilon^{-1} \boldsymbol{f}. \tag{15}$$

Observe that the number of equations in (15) is equal to $3 \times \#\mathcal{T}_h$, whereas the number of unknowns is equal to

$$\dim \boldsymbol{V}_h^0 + \dim N_h = 2 \times \#\mathcal{E}_h^0 + \#\mathcal{E}_h^\partial.$$

It was noted in [13] that these two numbers are equal, and as a result, (15) yields a square matrix system. The unique solvability of (15) will be proved in the next section by showing that $\boldsymbol{f} = \mathbf{0}$ gives $\boldsymbol{u}_h = \mathbf{0}$ and $\xi_h = 0$ for sufficiently small h (cf. Theorem 4.2).

Since $\operatorname{curl} \boldsymbol{u}_h$ and $\operatorname{\mathbf{curl}}_h \xi_h$ are piecewise constant, the equations of (15) imply that

$$\overline{\xi_h} = \overline{\mu^{-1}} \operatorname{curl} \boldsymbol{u}_h, \qquad \operatorname{\mathbf{curl}}_h \xi_h = \big(\overline{\epsilon^{-1}}\big)^{-1} \big(\omega^2\, \overline{\boldsymbol{u}_h} + \overline{\epsilon^{-1} \boldsymbol{f}}\,\big). \tag{16}$$

Using this result, we can eliminate either $\boldsymbol{u}_h$ or ξ_h from the mixed system (15) and recover it from the other variable. This feature is very helpful in implementing the mixed finite volume method (15) as well as in establishing its stability and error estimates by slight modification of the standard analysis, as will be shown in the next sections.

Elimination and recovery of $\boldsymbol{u}_h$: Rewriting (16) as

$$\operatorname{curl} \boldsymbol{u}_h = \big(\overline{\mu^{-1}}\big)^{-1} \overline{\xi_h}, \qquad \overline{\boldsymbol{u}_h} = \frac{1}{\omega^2} \big(\overline{\epsilon^{-1}} \operatorname{\mathbf{curl}}_h \xi_h - \overline{\epsilon^{-1} \boldsymbol{f}}\,\big), \tag{17}$$

we can eliminate the vector variable $\boldsymbol{u}_h$ from (15) and get an equation for the scalar variable ξ_h. Since $\operatorname{\mathbf{curl}}_h \chi_h$ is piecewise constant for $\chi_h \in N_h$, the second equation of (15) immediately gives

$$\begin{aligned} &\sum_{K \in \mathcal{T}_h} \left(\int_K \epsilon^{-1} \operatorname{\mathbf{curl}} \xi_h \cdot \operatorname{\mathbf{curl}} \chi_h - \omega^2 \int_K \boldsymbol{u}_h \cdot \operatorname{\mathbf{curl}} \chi_h \right) \\ &= \sum_{K \in \mathcal{T}_h} \int_K \epsilon^{-1} \boldsymbol{f} \cdot \operatorname{\mathbf{curl}} \chi_h. \end{aligned}$$

Using discrete Green's formula (12) and the first equality of (17), we obtain

$$\sum_{K \in \mathcal{T}_h} \int_K \boldsymbol{u}_h \cdot \operatorname{\mathbf{curl}} \chi_h = \int_\Omega \boldsymbol{u}_h \cdot \operatorname{\mathbf{curl}}_h \chi_h = \int_\Omega \operatorname{curl} \boldsymbol{u}_h \, \chi_h = \int_\Omega \big(\overline{\mu^{-1}}\big)^{-1} \overline{\xi_h} \chi_h.$$

Combining the two results above leads to the following equation for $\xi_h \in N_h$

$$\overline{a}(\xi_h, \chi_h) = F(\chi_h) \qquad \forall \chi_h \in N_h, \tag{18}$$

where

$$\overline{a}(\xi_h, \chi_h) = \int_\Omega \epsilon^{-1} \,\mathbf{curl}_h\, \xi_h \cdot \mathbf{curl}_h\, \chi_h - \omega^2 \int_\Omega \left(\overline{\mu^{-1}}\right)^{-1} \overline{\xi_h} \chi_h.$$

This is a modification of the standard $P1$ nonconforming FEM for the problem (5). In particular, when μ is piecewise constant, the lower-order term of (18) becomes

$$\omega^2 \int_\Omega \left(\overline{\mu^{-1}}\right)^{-1} \overline{\xi_h} \chi_h = \omega^2 \int_\Omega \mu \,\overline{\xi_h}\,\overline{\chi_h},$$

which is equivalent to applying one-point quadrature to $\omega^2 \int_K \mu\, \xi_h \chi_h$ on each element $K \in \mathcal{T}_h$.

After computing $\xi_h \in N_h$ by (18), we can use (17) and the equality (cf. (9))

$$\boldsymbol{u}_h = \overline{\boldsymbol{u}_h} - \frac{1}{2}(\mathrm{curl}\, \boldsymbol{u}_h) \boldsymbol{r}_h^\perp \tag{19}$$

to recover $\boldsymbol{u}_h \in \boldsymbol{V}_h^0$ in an element-by-element manner.

Elimination and recovery of ξ_h: We may first eliminate the scalar variable ξ_h from (15), get an equation for the vector variable $\boldsymbol{u}_h$, and then recover ξ_h from the computed $\boldsymbol{u}_h$. Indeed, since $\mathrm{curl}\, \boldsymbol{v}_h$ is piecewise constant for $\boldsymbol{v}_h \in \boldsymbol{V}_h^0$, using the first equation of (15) and then discrete Green's formula (12) yields

$$\int_\Omega \mu^{-1} \,\mathrm{curl}\, \boldsymbol{u}_h \,\mathrm{curl}\, \boldsymbol{v}_h = \int_\Omega \xi_h \,\mathrm{curl}\, \boldsymbol{v}_h = \int_\Omega \mathbf{curl}_h\, \xi_h \cdot \boldsymbol{v}_h. \tag{20}$$

Hence, by substituting the second equality of (16) into (20), we obtain for all $\boldsymbol{v}_h \in \boldsymbol{V}_h^0$

$$\int_\Omega \mu^{-1} \,\mathrm{curl}\, \boldsymbol{u}_h \,\mathrm{curl}\, \boldsymbol{v}_h - \omega^2 \int_\Omega \left(\overline{\epsilon^{-1}}\right)^{-1} \overline{\boldsymbol{u}_h} \cdot \boldsymbol{v}_h = \int_\Omega \left(\overline{\epsilon^{-1}}\right)^{-1} \overline{\epsilon^{-1} \boldsymbol{f}} \cdot \boldsymbol{v}_h. \tag{21}$$

This is a modification of the standard lowest-order Nédélec edge element method for the primal formulation (3). In particular, when ϵ is piecewise constant, the equation (21) is simplified to

$$\int_\Omega \mu^{-1} \,\mathrm{curl}\, \boldsymbol{u}_h \,\mathrm{curl}\, \boldsymbol{v}_h - \omega^2 \int_\Omega \epsilon\, \overline{\boldsymbol{u}_h} \cdot \boldsymbol{v}_h = \int_\Omega \overline{\boldsymbol{f}} \cdot \boldsymbol{v}_h,$$

and, analogously to (18), the lower-order term

$$\omega^2 \int_\Omega \epsilon\, \overline{\boldsymbol{u}_h} \cdot \boldsymbol{v}_h = \omega^2 \int_\Omega \epsilon\, \overline{\boldsymbol{u}_h} \cdot \overline{\boldsymbol{v}_h}$$

is obtained by applying one-point quadrature to $\omega^2 \int_K \epsilon\, \boldsymbol{u}_h \cdot \boldsymbol{v}_h$ on each element $K \in \mathcal{T}_h$. After solving for $\boldsymbol{u}_h \in \boldsymbol{V}_h^0$, we can readily recover $\xi_h \in N_h$ by combining (16) with the following equality

$$\xi_h = \overline{\xi_h} + (\mathbf{curl}_h\, \xi_h) \cdot \boldsymbol{r}_h^\perp.$$

Remark 3.1. From the viewpoint of error analysis, it seems more attractive to work with (18) after elimination of $\boldsymbol{u}_h$, because we can get a higher order of convergence for $\|\xi - \xi_h\|_0$ by applying the duality argument directly to (18).

Remark 3.2. The mixed finite volume method (15) can be extended to the nonhomogeneous boundary condition $\boldsymbol{u} \cdot \boldsymbol{t}|_{\partial\Omega} = g_D$ as follows: find $(\boldsymbol{u}_h, \xi_h) \in \boldsymbol{V}_h \times N_h$ such that $\boldsymbol{u}_h \cdot \boldsymbol{t}|_{\partial\Omega} = \overline{g_D}$ and (15) is satisfied for all $K \in \mathcal{T}_h$, where $\overline{g_D}|_e = \frac{1}{|e|} \int_e g_D$ for $e \in \mathcal{E}_h^\partial$. It is not difficult to verify that the variational formulation (5) for $\xi \in H^1(\Omega)$ holds with the modified right-hand side

$$F(\chi) = \int_\Omega \epsilon^{-1} \boldsymbol{f} \cdot \mathbf{curl}\, \chi - \omega^2 \int_{\partial\Omega} g_D \chi$$

and that the corresponding modification for the right-hand side of the $P1$ nonconforming FEM (18) is given by

$$\overline{F}(\chi_h) = \int_\Omega \epsilon^{-1} \boldsymbol{f} \cdot \mathbf{curl}_h\, \chi_h - \omega^2 \int_{\partial\Omega} \overline{g_D} \chi_h.$$

Numerical experiments suggest that the convergence orders of $\boldsymbol{u}_h$ and ξ_h do not deteriorate, at least for smooth g_D.

4. Stability analysis

In this section we show that the mixed finite volume method (15) admits a unique solution by establishing the stability estimate. Our strategy is to analyze the modified $P1$ nonconforming FEM (18) for ξ_h using the argument of [10] and then exploit the recovery formula (19) for $\boldsymbol{u}_h$. A minor difference with [10] is that the (homogeneous) Neumann boundary condition on $\partial\Omega$ is considered in (5) and (18), so we perform the analysis in terms of the broken H^1 norm $\|\cdot\|_{1,h}$ instead of the seminorm $|\cdot|_{1,h}$ as used in [10].

Since (5) is an indefinite problem, it is necessary to use the Aubin–Nitsche duality argument by considering the following dual problem of (5) (cf. [30,31]):

Given $g \in L^2(\Omega)$, find $\Phi \in H^1(\Omega)$ such that

$$a(\chi, \Phi) = \int_\Omega g\chi \qquad \forall \chi \in H^1(\Omega). \tag{22}$$

As mentioned in Section 1, the original problem (5) is well-posed when $\omega^2 \neq 0$ is not an interior Maxwell eigenvalue. Under the same condition, the dual problem (22) also has a unique solution satisfying

$$\|\Phi\|_1 \le C \|g\|_0. \tag{23}$$

Moreover, straightforward adaptations of [31, Theorem 2] and [10, Lemma 3.2] to the Neumann boundary condition show the following results: For any given $\delta > 0$,

- the $P1$ conforming finite element approximation Φ_C of Φ satisfies

$$\|\Phi - \Phi_C\|_1 \le \delta \|g\|_0, \tag{24}$$

- the consistency error of the dual problem satisfies

$$a(\chi_h, \Phi) - \int_\Omega g\chi_h \le C\delta \|g\|_0 \|\chi_h\|_{1,h} \qquad \forall \chi_h \in N_h, \tag{25}$$

provided that the mesh size h is sufficiently small.

Now we are ready to present the following lemma which establishes the stability of the standard $P1$ nonconforming FEM for the problem (5). This is a simple modification of [10, Theorem 3.1]. We remark that no regularity assumptions are made here on the solution $\xi \in H^1(\Omega)$ of the problem (5) and the solution $\Phi \in H^1(\Omega)$ of the dual problem (22).

Lemma 4.1. *Let G be a linear functional on N_h whose discrete H^{-1} norm is defined by*

$$\|G\|_{-1,h} = \sup_{\chi_h \in N_h} \frac{G(\chi_h)}{\|\chi_h\|_{1,h}}. \tag{26}$$

Then, for sufficiently small h, the solution $\psi_h \in N_h$ of the discrete problem

$$a(\psi_h, \chi_h) = G(\chi_h) \qquad \forall \chi_h \in N_h \tag{27}$$

satisfies the following stability estimate

$$\|\psi_h\|_{1,h} \le C\|G\|_{-1,h}.$$

Proof. The proof is essentially the same as the proof of [10, Theorem 3.1] and is included here for the reader's convenience.

Taking $\chi_h = \psi_h$ in (27) and applying Gårding's inequality (10), we obtain

$$\|\psi_h\|_{1,h} \le C(\|\psi_h\|_0 + \|G\|_{-1,h}). \tag{28}$$

Next we estimate $\|\psi_h\|_0$ by mean of the Aubin–Nitsche duality argument. Fix $g \in L^2(\Omega)$ and $\delta > 0$. Let $\Phi \in H^1(\Omega)$ be the solution of the dual problem (22) and let h be sufficiently small so that (24)-(25) hold. It is trivial to see that

$$\int_\Omega g\psi_h = \left\{ \int_\Omega g\psi_h - a(\psi_h, \Phi) \right\} + a(\psi_h, \Phi - \Phi_C) + G(\Phi_C).$$

The first term represents the consistency error of the dual problem which is bounded by (25)

$$\int_\Omega g\psi_h - a(\psi_h, \Phi) \le C\delta \|g\|_0 \|\psi_h\|_{1,h}.$$

The second term can be readily bounded by (10) and (24)

$$a(\psi_h, \Phi - \Phi_C) \le C\|\psi_h\|_{1,h} \|\Phi - \Phi_C\|_1 \le C\delta \|g\|_0 \|\psi_h\|_{1,h}.$$

Similarly, it follows by (26), (24) and (23) that

$$G(\Phi_C) \le \|G\|_{-1,h} \|\Phi_C\|_1 \le \|G\|_{-1,h} (\|\Phi_C - \Phi\|_1 + \|\Phi\|_1) \le C\|G\|_{-1,h} \|g\|_0.$$

Collecting the above results and taking $g = \psi_h$, we obtain

$$\|\psi_h\|_0 \le C(\delta \|\psi_h\|_{1,h} + \|G\|_{-1,h}),$$

which, when substituted into (28), gives

$$\|\psi_h\|_{1,h} \le C(\delta\|\psi_h\|_{1,h} + \|G\|_{-1,h}).$$

The proof is completed by choosing δ sufficiently small. $\square$

From Lemma 4.1 it is deduced that for sufficiently small h, the standard $P1$ nonconforming FEM for the problem (5)

$$a(\widehat{\xi}_h, \chi_h) = F(\chi_h) \qquad \forall \chi_h \in N_h \tag{29}$$

has a unique solution $\widehat{\xi}_h \in N_h$ satisfying

$$\|\widehat{\xi}_h\|_{1,h} \le C\|\boldsymbol{f}\|_0. \tag{30}$$

By further estimating $\|\widehat{\xi}_h - \xi_h\|_{1,h}$, we can prove the following stability result for the modified $P1$ nonconforming FEM (18) and the mixed finite volume method (15).

Theorem 4.2. *For sufficiently small h, the mixed finite volume method* (15) *has a unique solution $(\boldsymbol{u}_h, \xi_h) \in \boldsymbol{V}_h^0 \times N_h$ satisfying*

$$\|\boldsymbol{u}_h\|_{H(\mathrm{curl};\Omega)} + \|\xi_h\|_{1,h} \le C\|\boldsymbol{f}\|_0. \tag{31}$$

Proof. Since (15) is a square matrix system, its solvability follows from the uniqueness of the solution which is a direct consequence of (31). Let $\widehat{\xi}_h \in N_h$ be the solution of (29). To prove (31), we first note that

$$a(\widehat{\xi}_h - \xi_h, \chi_h) = G(\chi_h),$$

where

$$\begin{aligned} G(\chi_h) = F(\chi_h) - a(\xi_h, \chi_h) &= \overline{a}(\xi_h, \chi_h) - a(\xi_h, \chi_h) \\ &= \omega^2 \int_\Omega \{\mu\xi_h - (\overline{\mu^{-1}})^{-1}\overline{\xi_h}\}\chi_h. \end{aligned}$$

In order to apply Lemma 4.1, we need to estimate $\|G\|_{-1,h}$. Write $\frac{1}{\omega^2}G(\chi_h)$ as

$$\int_\Omega \{\mu\xi_h - (\overline{\mu^{-1}})^{-1}\overline{\xi_h}\}\chi_h = I + II,$$

where

$$I = \int_\Omega \{\mu - (\overline{\mu^{-1}})^{-1}\}\xi_h\chi_h, \qquad II = \int_\Omega (\overline{\mu^{-1}})^{-1}(\xi_h - \overline{\xi_h})\chi_h.$$

By the estimates (11) and the Cauchy–Schwarz inequality, it follows that

$$\begin{aligned} I &= \int_\Omega (\overline{\mu^{-1}})^{-1}\{\overline{\mu^{-1}} - \mu^{-1}\}\,\mu\,\xi_h\chi_h \\ &= \int_\Omega (\overline{\mu^{-1}})^{-1}\{\overline{\mu^{-1}} - \mu^{-1}\}(\mu\,\xi_h\chi_h - \overline{\mu\,\xi_h\chi_h}) \\ &= \int_\Omega (\overline{\mu^{-1}})^{-1}\{\overline{\mu^{-1}} - \mu^{-1}\} \end{aligned}$$

$$\times \left\{(\mu-\overline{\mu})\xi_h\chi_h + \overline{\mu}(\xi_h\chi_h - \overline{\xi_h\chi_h}) + \overline{(\overline{\mu}-\mu)\xi_h\chi_h}\right\}$$

$$\leq Ch^2\|\xi_h\|_{1,h}\|\chi_h\|_{1,h},$$

$$II = \int_\Omega \left(\overline{\mu^{-1}}\right)^{-1}(\xi_h - \overline{\xi_h})(\chi_h - \overline{\chi_h}) \leq Ch^2|\xi_h|_{1,h}|\chi_h|_{1,h},$$

which leads to

$$\|G\|_{-1,h} \leq Ch^2\|\xi_h\|_{1,h}.$$

Hence, by Lemma 4.1, we obtain

$$\|\widehat{\xi}_h - \xi_h\|_{1,h} \leq Ch^2\|\xi_h\|_{1,h}. \tag{32}$$

Combining (30) and (32) gives

$$\|\xi_h\|_{1,h} \leq \|\xi_h - \widehat{\xi}_h\|_{1,h} + \|\widehat{\xi}_h\|_{1,h} \leq Ch^2\|\xi_h\|_{1,h} + C\|\boldsymbol{f}\|_0,$$

from which we conclude that

$$\|\xi_h\|_{1,h} \leq C\|\boldsymbol{f}\|_0$$

for sufficiently small h. Finally, using (19) and (17), we obtain

$$\|\boldsymbol{u}_h\|_{H(\mathrm{curl};\Omega)} \leq C(\|\overline{\boldsymbol{u}_h}\|_0 + \|\operatorname{curl}\boldsymbol{u}_h\|_0) \leq C(\|\xi_h\|_{1,h} + \|\boldsymbol{f}\|_0) \leq C\|\boldsymbol{f}\|_0.$$

This completes the proof of (31). □

5. Error estimates

In this section we will derive optimal error estimates for the solution $(\boldsymbol{u}_h, \xi_h)$ of the mixed finite volume method (15). As in the previous section, the error analysis is performed first for ξ_h and then for $\boldsymbol{u}_h$ via the local recovery formula (19).

From (31) and (32) it follows immediately that

$$\|\widehat{\xi}_h - \xi_h\|_{1,h} \leq Ch^2\|\boldsymbol{f}\|_0. \tag{33}$$

Therefore optimal H^1 and L^2 error estimates for ξ_h can be obtained from the corresponding error estimates for the solution $\widehat{\xi}_h$ of the standard $P1$ nonconforming FEM (29). To this end, we assume that the solution of the dual problem (22) satisfies the following regularity estimate for some $\gamma \in (0,1]$

$$\|\Phi\|_{1+\gamma} \leq C\|g\|_0, \tag{34}$$

and adapt the proofs of [10] to the $P1$ nonconforming FEM (29).

Theorem 5.1. *Assume that $\boldsymbol{u} \in (H^s(\Omega))^2$ and $\xi \in H^{1+s}(\Omega)$ for $0 < s \leq 1$ and that the regularity estimate* (34) *holds for some $\gamma \in (0,1]$. Let $\xi_h \in N_h$ be the solution of the modified $P1$ nonconforming FEM* (18). *Then we have for sufficiently small h*

$$\|\xi - \xi_h\|_{1,h} \leq Ch^s(\|\boldsymbol{u}\|_s + \|\operatorname{curl}\boldsymbol{u}\|_0 + \|\xi\|_{1+s} + \|\boldsymbol{f}\|_0), \tag{35}$$

$$\|\xi - \xi_h\|_0 \leq Ch^{s+\gamma}(\|\boldsymbol{u}\|_s + \|\operatorname{curl}\boldsymbol{u}\|_0 + \|\xi\|_{1+s} + \|\boldsymbol{f}\|_0). \tag{36}$$

Proof. Let $\widehat{\xi}_h \in N_h$ be the solution of (29) and note that for all $\eta_h, \chi_h \in N_h$,

$$a(\eta_h - \widehat{\xi}_h, \chi_h) = a(\eta_h - \xi, \chi_h) + a(\xi, \chi_h) - F(\chi_h).$$

By (10) we have

$$a(\eta_h - \xi, \chi_h) \leq C\|\eta_h - \xi\|_{1,h}\|\chi_h\|_{1,h},$$

and

$$a(\xi, \chi_h) - F(\chi_h) \leq I_{ce}\|\chi_h\|_{1,h},$$

where I_{ce} is the consistency error given by

$$I_{ce} = \sup_{\chi_h \in N_h} \frac{a(\xi, \chi_h) - F(\chi_h)}{\|\chi_h\|_{1,h}}.$$

Then, by applying Lemma 4.1, it follows that

$$\|\eta_h - \widehat{\xi}_h\|_{1,h} \leq C(\|\xi - \eta_h\|_{1,h} + I_{ce}),$$

which results in

$$\|\xi - \widehat{\xi}_h\|_{1,h} \leq C\Big(\inf_{\eta_h \in N_h} \|\xi - \eta_h\|_{1,h} + I_{ce}\Big).$$

Choosing $\eta_h \in N_h$ to be the standard $P1$ nonconforming interpolant of ξ, we have

$$\inf_{\eta_h \in N_h} \|\xi - \eta_h\|_{1,h} \leq Ch^s\|\xi\|_{1+s}. \tag{37}$$

In order to estimate the consistency error I_{ce}, we slightly modify the proof of [10, Lemma 3.2] and employ the enriching operator $E : N_h \to H^1(\Omega)$ satisfying (13) and (14). Note that (5) and (4) yield

$$\begin{aligned}
a(\xi, \chi_h) - F(\chi_h) &= a(\xi, \chi_h - E\chi_h) - F(\chi_h - E\chi_h) \\
&= \int_\Omega \epsilon^{-1}\,\mathbf{curl}\,\xi \cdot \mathbf{curl}_h(\chi_h - E\chi_h) - \omega^2 \int_\Omega \mu\,\xi(\chi_h - E\chi_h) \\
&\quad - \int_\Omega \epsilon^{-1}\boldsymbol{f} \cdot \mathbf{curl}_h(\chi_h - E\chi_h) \\
&= \omega^2 \int_\Omega \boldsymbol{u} \cdot \mathbf{curl}_h(\chi_h - E\chi_h) - \omega^2 \int_\Omega \operatorname{curl}\boldsymbol{u}(\chi_h - E\chi_h).
\end{aligned}$$

By using (14) and (13), we obtain

$$\begin{aligned}
a(\xi, \chi_h) - F(\chi_h) &= \omega^2 \int_\Omega (\boldsymbol{u} - \overline{\boldsymbol{u}}) \cdot \mathbf{curl}_h(\chi_h - E\chi_h) - \omega^2 \int_\Omega \operatorname{curl}\boldsymbol{u}(\chi_h - E\chi_h) \\
&\leq C(\|\boldsymbol{u} - \overline{\boldsymbol{u}}\|_0 + h\|\operatorname{curl}\boldsymbol{u}\|_0)\|\chi_h\|_{1,h},
\end{aligned}$$

and thus

$$I_{ce} \leq C(\|\boldsymbol{u} - \overline{\boldsymbol{u}}\|_0 + h\|\operatorname{curl}\boldsymbol{u}\|_0) \leq Ch^s(\|\boldsymbol{u}\|_s + \|\operatorname{curl}\boldsymbol{u}\|_0).$$

Collecting the above results yields

$$\|\xi - \widehat{\xi}_h\|_{1,h} \leq Ch^s(\|\boldsymbol{u}\|_s + \|\operatorname{curl}\boldsymbol{u}\|_0 + \|\xi\|_{1+s}), \tag{38}$$

which, together with (33), proves the H^1 error estimate (35).

Now we turn to the L^2 error estimate (36). The regularity assumption (34) implies that (24)-(25) hold with $\delta = h^\gamma$, and following the duality argument given in the proof of [10, Theorem 3.3], one can show that

$$\|\xi - \widehat{\xi}_h\|_0 \le Ch^\gamma \|\xi - \widehat{\xi}_h\|_{1,h}.$$

The proof is completed by combining this estimate with (38) and (33). □

Remark 5.2. For the divergence-free source term ($\operatorname{div} \boldsymbol{f} = 0$), it was shown in [29, Proposition 2] that if μ and ϵ are smooth, then there exists $s > \frac{1}{2}$ such that

$$\|\boldsymbol{u}\|_s + \|\operatorname{curl} \boldsymbol{u}\|_s \le C\|\boldsymbol{f}\|_0.$$

In particular, we have $s = 1$ if Ω is convex. This regularity estimate also holds for some $s > 0$ in the case that μ and ϵ are piecewise smooth over a partition of Ω into finitely many subdomains and Ω is simply-connected; see [2, Theorem 5.1]. Furthermore, using the Helmholtz decomposition of $\boldsymbol{u}$ and the regularity result of the elliptic problem (cf. [2,29]), we can deduce that the above regularity estimate still holds when $\operatorname{div} \boldsymbol{f} \in H^{-1+s}(\Omega)$ and $\|\operatorname{div} \boldsymbol{f}\|_{-1+s}$ is added to $\|\boldsymbol{f}\|_0$.

Remark 5.3. It is easy to check that the regularity assumption $\xi \in H^{1+s}(\Omega)$ is only used in the approximation property (37), so Theorem 5.1 is still valid when ξ is piecewise H^{1+s} and $\|\xi\|_{1+s}$ is replaced by the broken norm

$$\|\xi\|_{1+s,h} = \left(\sum_{K \in \mathcal{T}_h} \|\xi\|^2_{1+s,K} \right)^{1/2}.$$

In two dimensions we have

$$|\,\mathbf{curl}\,\xi|_{s,K} = |\omega^2 \epsilon \boldsymbol{u} + \boldsymbol{f}|_{s,K} \le \omega^2 |\epsilon \boldsymbol{u}|_{s,K} + |\boldsymbol{f}|_{s,K} \le C|\boldsymbol{u}|_{s,K} + |\boldsymbol{f}|_{s,K},$$

which gives by (8)

$$\|\xi\|_{1+s,h} \le C(\|\boldsymbol{u}\|_s + \|\boldsymbol{f}\|_{s,h}).$$

In other words, ξ is piecewise H^{1+s} if $\boldsymbol{u} \in (H^s(\Omega))^2$ and $\boldsymbol{f}$ is piecewise H^s. This strongly indicates that, instead of directly computing $\mu^{-1} \operatorname{curl} \boldsymbol{u}_h$ as an approximation to $\xi = \mu^{-1} \operatorname{curl} \boldsymbol{u}$, it is more reasonable to use one-order higher finite elements for ξ_h than $\boldsymbol{u}_h$, as is done in the mixed finite volume method (15) and in [6]; see also Remark 5.5.

Finally, in the following theorem we derive the error estimate for $\boldsymbol{u}_h$ in the $\boldsymbol{H}(\mathrm{curl})$ norm.

Theorem 5.4. *Let $(\boldsymbol{u}_h, \xi_h)$ be the solution of the mixed finite volume method* (15)*. Then, under the assumptions of Theorem 5.1, we have*

$$\|\boldsymbol{u} - \boldsymbol{u}_h\|_0 \le Ch^s(\|\boldsymbol{u}\|_s + \|\operatorname{curl} \boldsymbol{u}\|_0 + \|\xi\|_{1+s} + \|\boldsymbol{f}\|_0), \tag{39}$$

$$\|\operatorname{curl}(\boldsymbol{u} - \boldsymbol{u}_h)\|_0 \le Ch^{\min(1,s+\gamma)}(\|\boldsymbol{u}\|_s + \|\operatorname{curl} \boldsymbol{u}\|_0 + \|\xi\|_{1+s} + \|\boldsymbol{f}\|_0). \tag{40}$$

Proof. By the second equation of (15), we have for $K \in \mathcal{T}_h$

$$\int_K \{\epsilon^{-1}\,\mathbf{curl}(\xi - \xi_h) - \omega^2(\boldsymbol{u} - \boldsymbol{u}_h)\} = 0,$$

which implies that

$$\|\overline{\boldsymbol{u} - \boldsymbol{u}_h}\|_{0,K} = \frac{1}{\omega^2|K|^{1/2}}\left|\int_K \epsilon^{-1}\,\mathbf{curl}(\xi - \xi_h)\right| \le C|\xi - \xi_h|_{1,K}.$$

Together with (19) and (17), this result gives

$$\begin{aligned}\|\boldsymbol{u} - \boldsymbol{u}_h\|_0 &\le \|\boldsymbol{u} - \overline{\boldsymbol{u}}\|_0 + \|\overline{\boldsymbol{u} - \boldsymbol{u}_h}\|_0 + Ch\|\operatorname{curl}\boldsymbol{u}_h\|_0 \\ &\le C(h^s\|\boldsymbol{u}\|_s + |\xi - \xi_h|_{1,h} + h\|\xi_h\|_0).\end{aligned}$$

The first result (39) then follows by applying (35) and (31).

On the other hand, using the first equality of (17), we obtain

$$\begin{aligned}\operatorname{curl}(\boldsymbol{u} - \boldsymbol{u}_h) &= \mu\xi - \big(\overline{\mu^{-1}}\big)^{-1}\overline{\xi_h} = \mu\big(\overline{\mu^{-1}}\big)^{-1}\big\{\overline{\mu^{-1}\xi} - \mu^{-1}\overline{\xi_h}\big\} \\ &= \mu\big(\overline{\mu^{-1}}\big)^{-1}\big\{\big(\overline{\mu^{-1}} - \mu^{-1}\big)\xi + \mu^{-1}(\xi - \overline{\xi}) + \mu^{-1}\,\overline{\xi - \xi_h}\big\},\end{aligned}$$

which gives by (11)

$$\|\operatorname{curl}(\boldsymbol{u} - \boldsymbol{u}_h)\|_0 \le C(h\|\xi\|_1 + \|\xi - \xi_h\|_0).$$

So the second result (40) is proved by applying (8) and (36). □

Remark 5.5. By comparing (36) with the following one obtained by (40)

$$\|\xi - \mu^{-1}\operatorname{curl}\boldsymbol{u}_h\|_0 \le C\|\operatorname{curl}\boldsymbol{u} - \operatorname{curl}\boldsymbol{u}_h\|_0 = O(h^{\min(1,s+\gamma)}),$$

we conclude that ξ_h provides a higher-order approximation to $\xi = \mu^{-1}\operatorname{curl}\boldsymbol{u}$ than $\mu^{-1}\operatorname{curl}\boldsymbol{u}_h$ if $s+\gamma > 1$ (which is true when the exact solution is sufficiently smooth). This is one of the benefits of the mixed finite volume method (15) based on the mixed system (4). In particular, for smooth μ and ϵ, we get the full convergence order $\|\xi - \xi_h\|_0 = O(h^2)$ when Ω is convex and $\boldsymbol{f}$ is piecewise H^1 (cf. Remarks 5.2–5.3). Such an approximation may be also obtained from the standard lowest-order edge element by using the averaging operator but under the conditions of superconvergence (almost uniform triangulations and higher regularity of $\boldsymbol{u}$); for example, see [21].

6. Numerical results

In this section we report some numerical results to support the theoretical results of the previous section. In all of the examples, we set $\omega = 1$ and the source term $\boldsymbol{f}$ is determined by the given exact solution $\boldsymbol{u}$.

Example 1. First we consider the constant coefficients $\mu = \epsilon = 1$ and the following smooth solution on the unit square $\Omega = (0,1)^2$

$$\boldsymbol{u}(x,y) = (\cos 2\pi x \sin \pi y, \sin \pi x \cos 2\pi y)$$

TABLE 1. Errors and convergence orders for Example 1

$1/h$	$\|\boldsymbol{u}-\boldsymbol{u}_h\|_0$	Order	$\|\operatorname{curl}(\boldsymbol{u}-\boldsymbol{u}_h)\|_0$	Order	$\|\xi-\xi_h\|_0$	Order
8	1.8926e–1	—	3.8013e–1	—	7.0220e–2	—
16	9.5551e–2	0.9861	1.9114e–1	0.9919	1.7747e–2	1.9843
32	4.7892e–2	0.9965	9.5698e–2	0.9980	4.4489e–3	1.9960
64	2.3960e–2	0.9991	4.7865e–2	0.9995	1.1130e–3	1.9990
128	1.1982e–2	0.9998	2.3934e–2	0.9999	2.7829e–4	1.9998
256	5.9912e–3	0.9999	1.1967e–2	1.0000	6.9576e–5	1.9999
512	2.9956e–3	1.0000	5.9838e–3	1.0000	1.7394e–5	2.0000

which satisfies the homogeneous Dirichlet boundary condition $\boldsymbol{u}\cdot\boldsymbol{t}=0$ on $\partial\Omega$. Note that $\operatorname{div}\boldsymbol{u}\neq 0$ and so $\operatorname{div}\boldsymbol{f}\neq 0$. The numerical solution $(\boldsymbol{u}_h,\xi_h)$ is computed on a sequence of uniform triangulations generated by first partitioning Ω into equal squares of width $h=2^{-k}$ and then dividing every square into two congruent right triangles with the diagonal of slope 1.

The numerical errors are reported in Table 1, where the convergence orders are numerically computed by

$$(\text{Order}) = \log_2 \frac{(\text{Error for } 2h)}{(\text{Error for } h)}.$$

It is clearly observed that the convergence orders in Table 1 are in perfect agreement with those of Theorems 5.1-5.4.

Example 2. In the second example we consider the variable coefficients

$$\mu(x,y)=\frac{1}{(1+xy)^2}, \qquad \epsilon(x,y)=1+x^2+y^2$$

and the exact solution is chosen to be

$$\boldsymbol{u}(x,y)=\left(\frac{\sin 2\pi y}{1+xy},\frac{\sin 2\pi x}{1+xy}\right)$$

on the unit square $\Omega=(0,1)^2$. The numerical computation is done with the same sequence of uniform triangulations used in Example 1. The numerical results of Table 2 show that the convergence orders are as good as in the case of constant coefficients.

Example 3. The third example involves the following nonsmooth solution on the L-shaped domain $\Omega=(-1,1)^2\setminus([0,1]\times[0,-1])$

$$\boldsymbol{u}(r,\theta)=\mathbf{curl}\left(r^{\frac{2}{3}}\cos\frac{2}{3}\theta+\frac{1}{\pi^3}\cos\pi x\cos\pi y\right)$$

with the coefficients $\mu=\epsilon=1$. Here (r,θ) denotes the polar coordinates. This solution satisfies $\boldsymbol{u}\cdot\boldsymbol{t}=0$ on the two line segments of $\partial\Omega$ meeting at the origin but $\boldsymbol{u}\cdot\boldsymbol{t}\neq 0$ on the remaining part of $\partial\Omega$. Although $\boldsymbol{u}\in(H^s(\Omega))^2$ for any

TABLE 2. Errors and convergence orders for Example 2

$1/h$	$\|\boldsymbol{u}-\boldsymbol{u}_h\|_0$	Order	$\|\operatorname{curl}(\boldsymbol{u}-\boldsymbol{u}_h)\|_0$	Order	$\|\xi-\xi_h\|_0$	Order
8	1.8820e–1	—	9.9720e–1	—	2.1377e–1	—
16	9.4805e–2	0.9892	4.9946e–1	0.9975	5.3910e–2	1.9874
32	4.7491e–2	0.9973	2.4983e–1	0.9994	1.3507e–2	1.9969
64	2.3757e–2	0.9993	1.2493e–1	0.9998	3.3785e–3	1.9992
128	1.1880e–2	0.9998	6.2467e–2	1.0000	8.4473e–4	1.9998
256	5.9401e–3	1.0000	3.1234e–2	1.0000	2.1119e–4	2.0000
512	2.9701e–3	1.0000	1.5617e–2	1.0000	5.2798e–5	2.0000

$0 < s < \frac{2}{3}$, $\xi = \operatorname{curl}\boldsymbol{u} = \frac{2}{\pi}\cos\pi x\cos\pi y$ is smooth. We also note that the regularity estimate (34) for the dual problem holds with $0 < \gamma < \frac{2}{3}$.

The first experiment is performed for a sequence of uniform triangulations generated by successive uniform refinement of the initial triangulation (with $h = 1$) shown in the left of Figure 1. Table 3 presents the numerical errors, showing that the convergence orders are again in perfect agreement with those of Theorems 5.1-5.4. From these results we conjecture that the nonhomogeneous Dirichlet boundary condition does not affect the convergence orders (at least when $\boldsymbol{u}\cdot\boldsymbol{t}$ is smooth on $\partial\Omega$).

In the second experiment we perform adaptive mesh refinement using the following (local) residual error estimator of [11] for $K \in \mathcal{T}_h$ (which was originally developed for the standard lowest-order edge element of Nédélec)

$$\eta_K^2 = h_K^2\|\boldsymbol{f}+\omega^2\epsilon\boldsymbol{u}_h\|_{0,K}^2+\sum_{e\subset\partial K\setminus\partial\Omega}\big(h_e\|[\![\mu^{-1}\operatorname{curl}\boldsymbol{u}_h]\!]\|_{0,e}^2+h_e\|[\![\omega^2\epsilon\boldsymbol{u}_h\cdot\boldsymbol{n}_e]\!]\|_{0,e}^2\big).$$

Here $[\![v]\!]$ denotes the jump of v across $e \in \mathcal{E}_h^0$ and $\boldsymbol{n}_e$ is a fixed unit normal vector to e. The initial triangulation is again the one shown in the left of Figure 1. We apply the simple maximum marking strategy which marks $K \in \mathcal{T}_h$ (and some more elements around K to avoid hanging nodes) for refinement if $\eta_K > \frac{1}{2}\max_{K'\in\mathcal{T}_h}\eta_{K'}$.

The adapted triangulations after five and ten mesh refinements are displayed in the middle and right of Figure 1, where we can see that the residual error estimator captures well the singularity of $\boldsymbol{u}$ at the origin. The numerical errors are plotted in Figure 2 which shows that $\|\xi-\xi_h\|_0$ decreases more rapidly than $\|\boldsymbol{u}-\boldsymbol{u}_h\|_0$ and $\|\operatorname{curl}(\boldsymbol{u}-\boldsymbol{u}_h)\|_0$ as the triangulation is refined. More precisely, by means of the least-squares fitting, it is found that the following optimal convergence orders are achieved in the asymptotic regime

$$\|\boldsymbol{u}-\boldsymbol{u}_h\|_0 = O(N^{-0.5}),$$
$$\|\operatorname{curl}(\boldsymbol{u}-\boldsymbol{u}_h)\|_0 = O(N^{-0.5}),$$
$$\|\xi-\xi_h\|_0 = O(N^{-1.0}),$$

where $N = \#\mathcal{E}_h$ denotes the number of edges in $\mathcal{T}_h$.

TABLE 3. Errors and convergence orders for Example 3

$1/h$	$\|\boldsymbol{u}-\boldsymbol{u}_h\|_0$	Order	$\|\operatorname{curl}(\boldsymbol{u}-\boldsymbol{u}_h)\|_0$	Order	$\|\xi-\xi_h\|_0$	Order
8	1.338e0–1	—	8.3833e–2	—	4.3828e–2	—
16	8.1497e–2	0.7153	3.9648e–2	1.0803	1.6629e–2	1.3982
32	5.0839e–2	0.6808	1.9154e–2	1.0496	6.4667e–3	1.3626
64	3.1965e–2	0.6695	9.3707e–3	1.0314	2.5420e–3	1.3471
128	2.0145e–2	0.6661	4.6207e–3	1.0200	1.0041e–3	1.3401
256	1.2701e–2	0.6654	2.2900e–3	1.0128	3.9749e–4	1.3369
512	8.0076e–3	0.6655	1.1386e–3	1.0081	1.5753e–4	1.3353

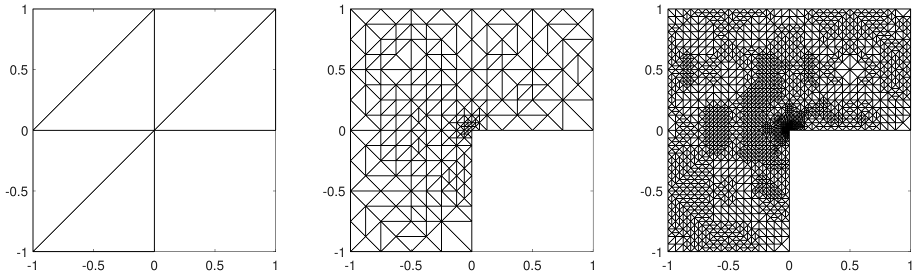

FIGURE 1. Initial (left) and adapted triangulations after five (middle) and ten (right) mesh refinement for Example 3

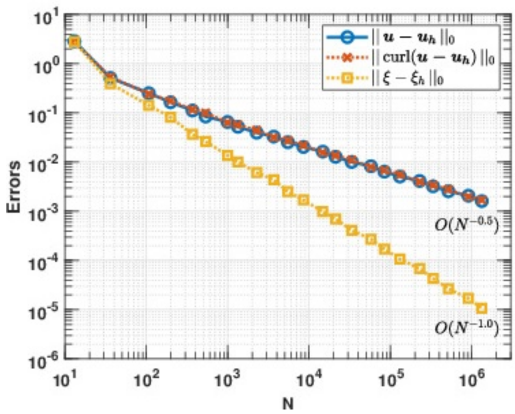

FIGURE 2. Errors and convergence orders for Example 3 with respect to the number of edges (N)

References

[1] D. Boffi, J. Guzmán, and M. Neilan, *Convergence of Lagrange finite elements for the Maxwell eigenvalue problem in two dimensions*, IMA J. Numer. Anal. **43** (2023), no. 2, 663–691. https://doi.org/10.1093/imanum/drab104

[2] A. Bonito, J.-L. Guermond, and F. Luddens, *Regularity of the Maxwell equations in heterogeneous media and Lipschitz domains*, J. Math. Anal. Appl. **408** (2013), no. 2, 498–512. https://doi.org/10.1016/j.jmaa.2013.06.018

[3] S. C. Brenner, *Two-level additive Schwarz preconditioners for nonconforming finite element methods*, Math. Comp. **65** (1996), no. 215, 897–921. https://doi.org/10.1090/S0025-5718-96-00746-6

[4] S. C. Brenner, *Convergence of nonconforming multigrid methods without full elliptic regularity*, Math. Comp. **68** (1999), no. 225, 25–53. https://doi.org/10.1090/S0025-5718-99-01035-2

[5] S. C. Brenner, *Poincaré-Friedrichs inequalities for piecewise H^1 functions*, SIAM J. Numer. Anal. **41** (2003), no. 1, 306–324. https://doi.org/10.1137/S0036142902401311

[6] S. C. Brenner, J. Cui, Z. Nan, and L. Sung, *Hodge decomposition for divergence-free vector fields and two-dimensional Maxwell's equations*, Math. Comp. **81** (2012), no. 278, 643–659. https://doi.org/10.1090/S0025-5718-2011-02540-8

[7] S. C. Brenner, F. Li, and L.-Y. Sung, *A locally divergence-free nonconforming finite element method for the time-harmonic Maxwell equations*, Math. Comp. **76** (2007), no. 258, 573–595. https://doi.org/10.1090/S0025-5718-06-01950-8

[8] S. C. Brenner, F. Li, and L.-Y. Sung, *A locally divergence-free interior penalty method for two-dimensional curl-curl problems*, SIAM J. Numer. Anal. **46** (2008), no. 3, 1190–1211. https://doi.org/10.1137/060671760

[9] S. C. Brenner and L.-Y. Sung, *A quadratic nonconforming vector finite element for $H(\mathrm{curl};\Omega)\cap H(\mathrm{div};\Omega)$*, Appl. Math. Lett. **22** (2009), no. 6, 892–896.

[10] C. Carstensen, A. K. Dond, N. Nataraj, and A. K. Pani, *Error analysis of nonconforming and mixed FEMs for second-order linear non-selfadjoint and indefinite elliptic problems*, Numer. Math. **133** (2016), no. 3, 557–597. https://doi.org/10.1007/s00211-015-0755-0

[11] C. Carstensen and R. H. W. Hoppe, Convergence analysis of an adaptive edge finite element method for the 2D eddy current equations, J. Numer. Math. **13** (2005), no. 1, 19–32. https://doi.org/10.1163/1569395054069017

[12] S.-H. Chou, D. Y. Kwak, and K. Y. Kim, *Mixed finite volume methods on nonstaggered quadrilateral grids for elliptic problems*, Math. Comp. **72** (2003), no. 242, 525–539. https://doi.org/10.1090/S0025-5718-02-01426-6

[13] B. Courbet and J.-P. Croisille, *Finite volume box schemes on triangular meshes*, RAIRO Modél. Math. Anal. Numér. **32** (1998), no. 5, 631–649. https://doi.org/10.1051/m2an/1998320506311

[14] M. Crouzeix and P.-A. Raviart, *Conforming and nonconforming finite element methods for solving the stationary Stokes equations. I*, R.A.I.R.O. **7** (1973), no. R-3, 33–75.

[15] T. Gudi, *A new error analysis for discontinuous finite element methods for linear elliptic problems*, Math. Comp. **79** (2010), no. 272, 2169–2189. https://doi.org/10.1090/S0025-5718-10-02360-4

[16] P. Hansbo and T. Rylander, *A linear nonconforming finite element method for Maxwell's equations in two dimensions. Part I: frequency domain*, J. Comput. Phys. **229** (2010), no. 18, 6534–6547. https://doi.org/10.1016/j.jcp.2010.05.009

[17] R. Hiptmair, *Finite elements in computational electromagnetism*, Acta Numer. **11** (2002), 237–339. https://doi.org/10.1017/S0962492902000041

[18] P. Houston, I. Perugia, A. Schneebeli, and D. Schötzau, *Interior penalty method for the indefinite time-harmonic Maxwell equations*, Numer. Math. **100** (2005), no. 3, 485–518. https://doi.org/10.1007/s00211-005-0604-7

[19] P. Houston, I. Perugia, A. Schneebeli, and D. Schötzau, *Mixed discontinuous Galerkin approximation of the Maxwell operator: the indefinite case*, M2AN Math. Model. Numer. Anal. **39** (2005), no. 4, 727–753. https://doi.org/10.1051/m2an:2005032

[20] D. Y. Kwak, *A new class of higher order mixed finite volume methods for elliptic problems*, SIAM J. Numer. Anal. **50** (2012), no. 4, 1941–1958. https://doi.org/10.1137/100812446

[21] J. Li, Y. Huang, and W. Yang, *An adaptive edge finite element method for electromagnetic cloaking simulation*, J. Comput. Phys. **249** (2013), 216–232. https://doi.org/10.1016/j.jcp.2013.04.026

[22] J.-M. Mirebeau, *Nonconforming vector finite elements for $H(\mathrm{curl};\Omega)\cap H(\mathrm{div};\Omega)$*, Appl. Math. Lett. **25** (2012), no. 3, 369–373.

[23] P. Monk, *A finite element method for approximating the time-harmonic Maxwell equations*, Numer. Math. **63** (1992), no. 2, 243–261. https://doi.org/10.1007/BF01385860

[24] P. Monk, *Finite Element Methods for Maxwell's Equations*, Numerical Mathematics and Scientific Computation, Oxford Univ. Press, New York, 2003. https://doi.org/10.1093/acprof:oso/9780198508885.001.0001

[25] P. Monk, *A simple proof of convergence for an edge element discretization of Maxwell's equations*, Computational electromagnetics (Kiel, 2001), 127–141, Lect. Notes Comput. Sci. Eng., 28, Springer, Berlin, 2003. https://doi.org/10.1007/978-3-642-55745-3_9

[26] J. C. Nédélec, *Mixed finite elements in* $\mathbf{R}^3$, Numer. Math. **35** (1980), no. 3, 315–341. https://doi.org/10.1007/BF01396415

[27] J. C. Nédélec, *A new family of mixed finite elements in* $\mathbf{R}^3$, Numer. Math. **50** (1986), no. 1, 57–81. https://doi.org/10.1007/BF01389668

[28] N. C. Nguyen, J. Peraire, and B. Cockburn, *Hybridizable discontinuous Galerkin methods for the time-harmonic Maxwell's equations*, J. Comput. Phys. **230** (2011), no. 19, 7151–7175. https://doi.org/10.1016/j.jcp.2011.05.018

[29] I. Perugia, D. Schötzau, and P. Monk, *Stabilized interior penalty methods for the time-harmonic Maxwell equations*, Comput. Methods Appl. Mech. Engrg. **191** (2002), no. 41-42, 4675–4697. https://doi.org/10.1016/S0045-7825(02)00399-7

[30] A. H. Schatz, *An observation concerning Ritz-Galerkin methods with indefinite bilinear forms*, Math. Comp. **28** (1974), 959–962. https://doi.org/10.2307/2005357

[31] A. H. Schatz and J. Wang, *Some new error estimates for Ritz-Galerkin methods with minimal regularity assumptions*, Math. Comp. **65** (1996), no. 213, 19–27. https://doi.org/10.1090/S0025-5718-96-00649-7

[32] L. Zhong, S. Shu, G. Wittum, and J. Xu, *Optimal error estimates for Nedelec edge elements for time-harmonic Maxwell's equations*, J. Comput. Math. **27** (2009), no. 5, 563–572. https://doi.org/10.4208/jcm.2009.27.5.011

Kwang-Yeon Kim
Department of Mathematics
Kangwon National University
Chuncheon 24341, Korea
Email address: eulerkim@kangwon.ac.kr

Do Young Kwak
Department of Mathematical Sciences
Korea Advanced Institute of Science and Technology
Daejeon 34141, Korea
Email address: kdy@kaist.ac.kr